Thermal Fluctuations Between Conformational Substates of the Fe^{2+}-His^{F8} Linkage in Deoxymyoglobin Probed by the Raman Active Fe-N_ϵ(His^{F8}) Stretching Vibration

Harald Gilch, Wolfgang Dreybrodt, and Reinhard Schweitzer-Stenner
FB1-Institut für Experimentelle Physik, Universität Bremen, 28334 Bremen, Germany

ABSTRACT We have measured the $\nu_{Fe\text{-}His}$ Raman band of horse heart deoxymyoglobin dissolved in an aqueous solution as a function of temperature between 10 and 300 K. The minimal model to which these data can be fitted in a statistically significant and physically meaningful way comprises four different Lorentzian bands with frequencies at 197, 209, 218, and 226 cm^{-1}, and a Gaussian band at 240 cm^{-1}, which exhibit halfwidths between 10 and 12.5 cm^{-1}. All these parameters were assumed to be independent of temperature. The temperature dependence of the apparent total band shape's frequency is attributed to an intensity redistribution of the subbands at $\Omega_1 = 209$ cm^{-1}, $\Omega_2 = 218$ cm^{-1}, and $\Omega_3 = 226$ cm^{-1}, which are assigned to Fe-N_ϵ(His^{F8}) stretching modes in different conformational substates of the Fe-His^{F8} linkage. They comprise different out-of-plane displacements of the heme iron. The two remaining bands at 197 and 240 cm^{-1} result from porphyrin modes. Their intensity ratio is nearly temperature independent. The intensity ratio I_3/I_2 of the $\nu_{Fe\text{-}His}$ subbands exhibits a van't Hoff behavior between 150 and 300 K, bending over in a region between 150 and 80 K, and remains constant between 80 and 10 K, whereas I_2/I_1 shows a maximum at 170 K and approaches a constant value at 80 K. These data can be fitted by a modified van't Hoff expression, which accounts for the freezing into a non-equilibrium distribution of substates below a distinct temperature T_f and also for the linear temperature dependence of the specific heat of proteins. The latter leads to a temperature dependence of the entropic and enthalpic differences between conformational substates. The fits to the intensity ratios of the $\nu_{Fe\text{-}His}$ subbands yield a freezing temperature of $T_f = 117$ K and a transition region of $\Delta T = 55$ K. In comparison we have utilized the above thermodynamic model to reanalyze earlier data on the temperature dependence of the ratio A_0/A_1 of two subbands underlying the infrared absorption band of the CO stretching vibration in CO-ligated myoglobin (A. Ansari, J. Berendzen, D. Braunstein, B. R. Cowen, H. Frauenfelder, M. K. Kong, I. E. T. Iben, J. Johnson, P. Ormos, T. B. Sauke, R. Scholl, A. Schulte, P. J. Steinbach, R. D. Vittitow, and R. D. Young, 1987, *Biophys. Chem.* 26:237–335). This yields thermodynamic parameters, in particular the freezing temperature ($T_f = 231$ K) and the width of the transition region ($\Delta T =$ 8 K), which are significantly different from the corresponding parameters obtained from the above $\nu_{Fe\text{-}His}$ data, but very close to values describing the transition of protein bound water from a liquid into an amorphous state. These findings and earlier reported data on the temperature dependence exhibited by the Soret absorption bands of various deoxy and carbonmonoxymyoglobins led us to the conclusion that the fluctuations between conformational substates of the heme environment in carbonmonoxymyoglobin are strongly coupled to motions within the hydration shell, whereas the thermal motions between the substates of the Fe-His^{F8} linkage in deoxymyoglobin proceed on an energy landscape that is mainly determined by the intrinsic properties of the protein. The latter differ from protein fluctuations monitored by Mössbauer experiments on deoxymyoglobin crystals which exhibit a strong coupling to the protein bound water and most probably reflect a higher tier in the hierarchical arrangement of substates and equilibrium fluctuations.

INTRODUCTION

It is widely appreciated that myoglobin (Mb) serves as an ideal model system to study the complex relationship between structure, dynamics, and function of proteins. At first sight it seems that its function solely comprises a comparatively simple, reversible, bimolecular chemical reaction, namely the binding of small ligands as dioxygen (O_2) and carbon monoxide (CO) to the central atom of its heme group (Antonini and Brunori, 1970; Stryer, 1988). Numerous flash photolysis experiments, however, have provided evidence that these binding processes are more complicated (Austin et al., 1975; Doster et al., 1982; Ansari et al., 1987; Steinbach et al., 1991; Post et al., 1993). First, they proceed on a complex potential surface with multiple wells along the reaction coordinate (Austin et al., 1975; Steinbach et al., 1991). Geminate rebinding of photodissociated ligands at cryogenic temperatures is inhomogenous because it encounters slightly different enthalpic barriers in different molecules (Austin et al., 1975). This has been interpreted by assuming that the protein exist in different conformational substates in which it performs the same function at different rates (Frauenfelder et al., 1979, 1988). Time-resolved resonance Raman, kinetic hole-burning, and flash photolysis experiments have further shown that the protein undergoes various relaxation processes after photodissociation of its heme-bound ligand (Campbell et al., 1987; Chavez et al., 1990; Ahmed et al., 1991; Šrajer et al., 1988; Champion, 1992; Steinbach et al., 1991; Mourant et al., 1993).

Received for publication 8 July 1994 and in final form 11 April 1995.

Address reprint requests to Reinhard Schweitzer-Stenner, FB1-Institut für Experimentelle Physik, Universität Bremen, P. O. Box 330440, 28334 Bremen, Germany. Tel.: 49-421-218-2509; Fax: 49-421-218-3601; E-mail: stenner@theo.physik.uni-bremen.de.

0006-3495/95/07/214/14 $2.00

The most peculiar conclusion drawn from some of the above experiments is that proteins behave to some extent like glasses (Iben et al., 1989). Frauenfelder and co-workers have shown that the relaxation of non-equilibrium states of Mb induced by sudden changes of pressure or temperature have to be described by stretched rather than by single exponentials (Iben et al., 1989; Frauenfelder et al., 1990). This is characteristic for α-relaxations in glasses (Götze and Sjörgen, 1992). The thermal fluctuations between conformational substates (CSs) slow down below a distinct temperature yielding a freezing of the protein into a non-equilibrium distribution of its CS. This behavior is typical for frustrated systems such as spin glasses (Stein, 1985; Austin and Chen, 1992). Moreover, some experimental evidence is provided that similar to the situation in spin glasses the CSs of Mb are arranged in a hierarchy, i.e., each CS is further subdivided into different CSs of a higher tier (Ansari et al., 1985; Iben et al., 1989; Frauenfelder et al., 1990; Ahmed et al., 1991; Bosenbeck et al., 1992). Thus the relationship of CS in such a hierarchy may be visualized by a tree, whose branches are connecting different CSs belonging to adjacent tiers (Austin and Chen, 1992). Energy barriers between CS and as a consequence also the freezing temperature decrease with increasing tier.

For proteins the situation becomes even more complicated by their interactions with the solvent. Molecular dynamics simulations suggest strong coupling between fluctuations in Mb and in its hydration shell (Loncharich and Brooks, 1990; Steinbach and Brooks, 1993) which still exhibit a significant mobility of its water molecules (Steinhoff et al., 1993). This is in accordance with results from Mössbauer and microwave experiments on metMb crystals which show that the dielectric relaxation of crystal water and the mean square displacement of the heme iron exhibit a similar dependence on temperature even though they reflect processes proceeding on different time scales (Singh et al., 1981; Parak, 1986). Such a similarity between different relaxation processes in the same system is again typical for α-relaxations in glasses (Götze and Sjörgen, 1992). Lowering the temperature below the glass transition of the solvent results in a complete freezing of the protein (Parak et al., 1982; Frauenfelder and Gratton, 1986). However, owing to the above mentioned hierarchical arrangement of the CS into different tiers one may suspect that fluctuations between CS of high tiers may still be operative below this freezing temperature (Ansari et al., 1985; Ahmed et al., 1991).

Spectroscopic markers are frequently used to obtain information on the local structure associated with distinct CS and to probe thermal and non-equilibrium fluctuations between CS. First, the infrared (IR) band resulting from the CO-stretching mode (COs) of the heme-bound CO in sperm whale Mb was decomposed into three different subbands (Makinen et al., 1979), which were attributed to different CS (Ansari et al., 1987; Morikis et al., 1989). Kinetic and relaxation experiments have revealed that each of these CSs comprises other CSs of higher tiers with lower energy barriers (Ansari et al., 1987; Iben et al., 1989). The subbands were originally assigned to three different CO orientations with respect to the heme normal (Ormos et al., 1988), but this notion has recently been challenged by IR linear dichromism measurements on single crystals (Ivanov et al., 1994). Another spectral marker, which is more sensitive to the proximal environment of the heme is the so-called band III appearing at 760 nm in the optical spectrum of deoxyMb and deoxyhemoglobin. This band most probably results from an a_{2u}(heme) $\rightarrow$ 2 d_{xz}(Fe) charge transfer transition (Eaton et al., 1978). It has been shown to be inhomogenously broadened (Campbell et al., 1987; Šrajer and Champion, 1991). The apparent frequency position of the band depends at least in part on a protein coordinate, which also determines the barrier-controlling ligand rebinding from the heme pocket to the heme iron (Steinbach et al., 1991; Nienhaus et al., 1992, 1994). The third of the commonly used spectral markers is the Raman band resulting from the Fe-N_ϵ (His^{F8}) stretching mode ($\nu_{Fe\text{-}His}$), which appears at $\sim$220 cm^{-1} in the spectra of deoxygenated Mb and Hb (Kitagawa, 1988). In hemoglobin derivatives its peak position shifts toward higher frequencies upon changes from T-like to R-like quaternary structures (Rousseau and Friedman, 1988). We have recently shown that this rather broad band can be resolved into five Lorentzian subbands at 195, 202, 210, 218, and 226 cm^{-1}, which vary their intensities upon external perturbations such as changes of pH; phosphate concentration; and temperature, chemical modifications, or exchange of amino acid residues by natural or site-directed mutagenesis (Gilch et al., 1993). The frequencies and halfwidths of these subbands, however, were found to be practically unaffected by the above perturbations. The subbands were assigned to different CSs of the Fe-His^{F8} complex, which differ in terms of geometrical parameters, most likely the iron displacement δ and the tilt angle θ between the Fe-N_ϵ bond and the heme normal. They determine both frequencies and intensities of the subbands (Friedman et al., 1990; Stavrov, 1993; Stavrov and Kushkuley, 1993). Variations in the intensity of these bands by external perturbations may reflect a redistribution of the respective CS and/or changes in the intrinsic Raman cross section of their $\nu_{Fe\text{-}His}$. The latter is normally assigned to variations of the azimuthal angle φ between the projection of the Fe-N_ϵ bond onto the heme and its N(I)-Fe-N(III) line (Friedman et al., 1990; Ahmed et al., 1991; Bosenbeck et al., 1992).

Structural heterogenity of the Fe-His^{F8} linkage is also observed in the deoxygenated state of the less complex horse heart and sperm whale Mb. Their $\nu_{Fe\text{-}His}$ band exhibit three subbands at 209, 218, and 226 cm^{-1}. Upon lowering the temperature of horse heart Mb in an aqueous solution the two bands at lower frequencies decrease in intensity, whereas the high frequency band increases its intensity significantly (Gilch et al., 1993). As in deoxyHbA, positions and halfwidths of the subbands remain unaffected by temperature variations.

In the present study we measured the intensities of the $\nu_{\text{Fe-His}}$ subbands of horse heart deoxyMb as a function of temperature. From these data we obtain the differences in enthalpy and entropy between the corresponding CS and determine the transition temperature below which the CSs are frozen into a non-equilibrium distribution. Moreover, we compare our results with similar experiments on the IR CO band of sperm whale MbCO by Ansari et al. (1987), and Mössbauer experiments on deoxy sperm whale Mb (Parak et al., 1982). Thus we elucidate some interesting differences between the energy landscape of the heme environment in the non-ligated and ligated states of Mb and provide further evidence that CS of Mb are arranged in a hierarchical order.

MATERIALS AND METHODS

Preparation of the material

Horse heart Mb in lyophilized form was commercially obtained from Sigma Chemical Co. (St. Louis, MO) and was used without further purification. The pH value of the sample was adjusted to 7.2 by dialyzing against 0.05 M potassium phosphate buffer. The concentration (2 mM) of each sample was determined by measuring the absorbance with a HP-diode array spectrometer. By adding a few grains of sodium dithionite, each sample attained the deoxy state. To avoid oxygenation anaerobic conditions were maintained throughout the experiment.

Experimental setup

The low frequency spectra of deoxyMb (i.e., 100–400 cm^{-1}) were obtained using the 441 nm line of an He-Cd laser (Omnichrome, Cinho, CA) at an average power of 30 mW. Raman scattering was measured in the backscattering configuration. The laser beam, polarized perpendicular to the scattering plane, was focused by a cylindrical lens of 10 cm focal length onto the sample, which was situated in a low temperature metacrylate cell with one quartz window. The cell was mounted onto the cold finger of a Leybold Heraeus (Köln, Germany) closed cycle refrigerator, the temperature of which was regulated by a Leybold-Controller unit (Gilch, 1994). The scattered light was dispersed by a SPEX 1401 monochromator (SPEX Industries, Edison, NJ). Its entrance and exit slit widths were adjusted to 100 μm. This provides a spectral resolution of 2.5 cm^{-1} as derived from the profile of the plasma line appearing in the Raman spectrum at 283 cm^{-1}. Most of the data sets were recorded with a spectrometer speed of 0.03 cm^{-1}/s and a sampling time of 10 s.

Analysis of the line profiles

The line profiles of the $\nu_{\text{Fe-His}}$ bands were analyzed by using the programs SpectraCalc, purchased from Photometrix (Munich, Germany), and MULTIFIT, developed in our own laboratory. After subtracting the Rayleigh background we decomposed the profile alternatively into 3, 4, and 5 Lorentzian, Voigtian, or Gaussian subbands with adjustable frequencies, halfwidths, and heights. The frequency values were determined with an accuracy of ± 1 cm^{-1} by use of the 447.2 nm plasma line provided by the He-Cd laser, which appears in the Raman spectrum at 282.8 cm^{-1}. The apparent halfwidth of the subbands was always found to be by more than a factor of 4 larger than the spectral resolution so that a deconvolution of the spectrometer function was not necessary (Jentzen, 1994).

To investigate the reliability of the fits we first employed a method proposed by Grinvald and Steinberg (1974), who used the autocorrelation function of the residuals of a fit to judge its quality. This function $C(j)$ is given by:

$$C(j) = \sum_{i=1}^{m} (\delta_i \delta_{i+j}/m) / \sum_{i=1}^{n} (\delta_i^2/n) \quad (1)$$

δ_i is the difference between the fit function and the experimentally observed value. n is the number of data points and $m = n/2$. The autocorrelation function contains high frequency fluctuations because of noise in the spectra and low frequency deviations about zero, which reflects systematic non-random deviations of the fit function from the real physical wavenumber dependence of the Raman band.

Second, to determine the statistical significance of the fits, we calculated the reduced χ^2 function:

$$\chi_r^2 = \sum_i (\delta_i^2/(\sigma_i^2 \nu)) \quad (2)$$

where

$$\nu = N - k + 1$$

is the degree of freedom, σ_i is the standard deviation of each data point i estimated from the spectral noise, N is the number of data points, and k the number of free parameters used in the fit. In the case of an ideal fit χ_r^2 should be 1, since the expectation value of the χ^2 distribution is equal to ν. For large ν the variance of the χ^2 distribution is 2ν (Hays and Winkler, 1970). Thus the confidence interval for χ_r^2 lies between 0 and 2. However, χ_r^2 values <1 would indicate that the fit is better than is expected from the standard deviations of the data points. In that case features have been reproduced by the fit that are statistically not significant. Therefore only χ_r^2-values between 1 and 2 are indicative of reliable fitting (Bevington, 1969).

RESULTS

We measured the $\nu_{\text{Fe-His}}$ Raman profiles at various temperatures by adopting the following protocol. The aqueous sample of deoxyMb was cooled down at a rate of ~3 K/min to the desired temperature, which was kept constant for 10 min. The spectrum was then recorded within 15 min. A spectrum subsequently measured at the same temperature did not reveal any spectral changes. This indicates fast transitions between the substates at high temperatures and a sudden freeze-in at low temperatures. After the last spectrum of this series was recorded at 10 K, the cryostat was warmed up and the spectra were remeasured at the same temperatures used for the measurements during the cooling procedure. This yielded a good reproduction of the band profiles observed before, thus providing evidence that no irreversible processes are involved. Four of these band profiles recorded at 300, 250, 200, 150, 100, and 10 K are displayed in Fig. 1. They clearly illustrate the temperature dependence of the $\nu_{\text{Fe-His}}$ band. The peak frequency shifts with decreasing temperature from 219 cm^{-1} at 300 K to 222 cm^{-1} at 200 K and to 225 cm^{-1} at 100 and 10 K, in accordance with earlier results reported by Ahmed et al. (1991).

To obtain an optimal fit we proceeded as follows. We first tried to fit the data with three Lorentzian bands, which is the minimal number as indicated by the shoulders of the profiles. The halfwidths were kept equal within 2 cm^{-1} in

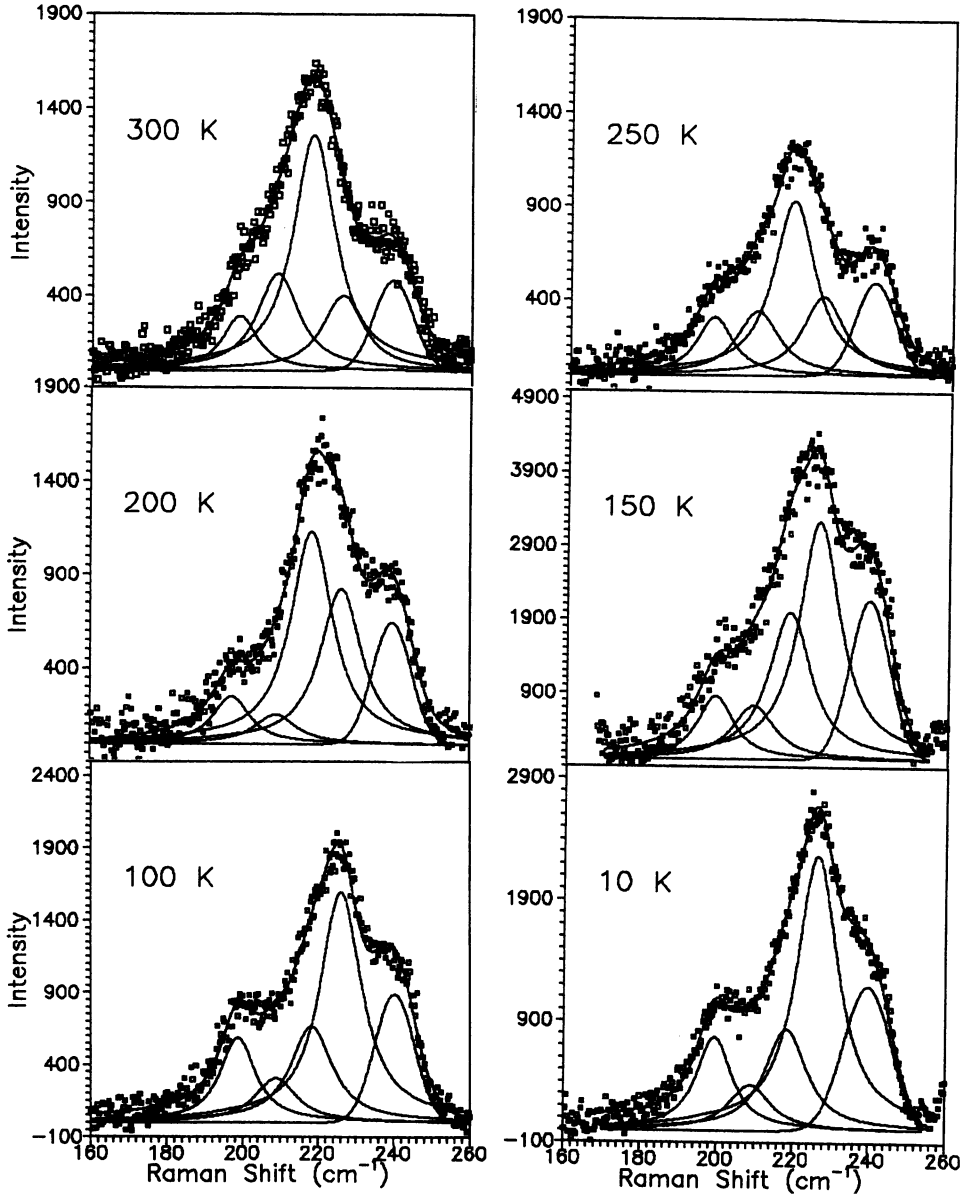

FIGURE 1 Band profiles of the $\nu_{\text{Fe-His}}$ band of horse heart deoxyMb measured at the indicated temperatures. The profiles were decomposed into five subbands by a procedure outlined in the text. The three central bands are attributed to the $\nu_{\text{Fe-His}}$ mode in different conformational substates.

line with earlier results on a variety of $\nu_{\text{Fe-His}}$ bands of various hemoglobin derivatives and mutants (Bosenbeck et al., 1992; Gilch et al., 1993). The fitting was then repeated with 4, 5, 6, and 7 bands. To check the quality of these fits the corresponding autocorrelation function $C_k(i)$ was computed according to Eq. 1 (k labels the number of Lorentzian sublines utilized in the fit). In a final step we calculated the differences $C_{k+1}(i)-C_k(i)$. Thus the random noise is eliminated and only systematic deviations due to imperfect fitting remain. As shown in Fig. 2 for the $\nu_{\text{Fe-His}}$ band taken at 300 K, these deviations decrease with increasing k and do not improve further for $k > 5$. This leads us to the conclusion that five bands are necessary for an appropriate fitting. The $\nu_{\text{Fe-His}}$ band of Mb, however, is less structured than that of hemoglobin derivatives, and an eyeballing of the band profiles shown in Fig. 1 suggests that a fit with three rather broad (inhomogenously broadened) bands may already suffice. Therefore we have tried to fit all data sets using three Gaussian subbands without any restriction for the halfwidths and frequencies (three-band (3b) model with nine free-fitting parameters). Indeed, we obtained satisfactory fits for all data sets. For example, Fig. 3 *a* shows the fit to the $\nu_{\text{Fe-His}}$ band taken at 200 K. The first column of Table 1 lists the corresponding χ_r^2 values for the fits to seven band profiles. All values are significantly <2. Some are even <1, suggesting that they are too good.

These fits yield a clear temperature dependence of the frequency of the central band, which decreases from 226 at 10 K to 218 cm^{-1} at 300 K (Fig. 3 *b*). Its halfwidth (i.e., 22 cm^{-1}) is quite large and practically independent of temperature. The room temperature frequencies of the remaining bands are 199 and 239 cm^{-1}; the corresponding halfwidths are 19 and 12 cm^{-1}. The 199 cm^{-1} band does not significantly change its frequency and halfwidth with temperature.

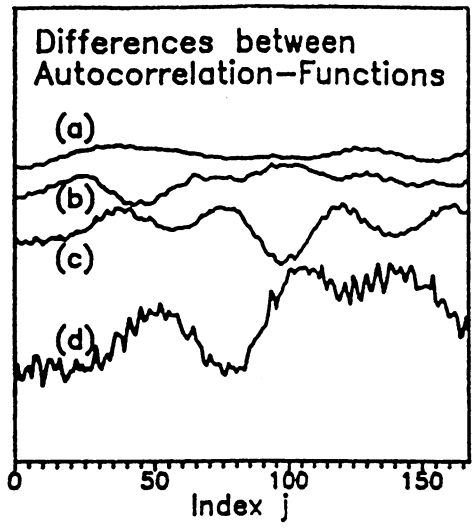

FIGURE 2 Plot of the differences between the autocorrelation functions obtained from the fits to the band profile measured at 300 K using 3 and 4 (*d*), 4 and 5 (*c*), 5 and 6 (*b*), and 6 and 7 (*a*) sublines. The autocorrelation function has been calculated by use of Eq. 1. The indices *j* from 0 to 174 cover the spectral region between 160 and 260 cm^{-1}.

The frequency of the 239 cm^{-1} band shifts slightly up with decreasing temperature (242 cm^{-1} at 10 K), whereas its halfwidth is somewhat reduced (10 cm^{-1} at 10 K).

One may suspect that the temperature dependence of the frequency of the central band (Fig. 3 *b*) can be rationalized by invoking anharmonic coupling between $\nu_{Fe\text{-}His}$ and lower frequency modes of the porphyrin or the protein environment. (J. T. Sage and P. M. Champion, personal communications). To check this possibility we have utilized a model that describes vibrational phase relaxation in terms of anharmonic coupling to a bath of low frequency modes (Perrson and Ryberg, 1989). For reasons of simplicity the latter was represented by one effective mode. Such a model has recently been employed to analyze the temperature dependence of porphyrin Raman lines (Asher and Murtaugh, 1983; Schweitzer-Stenner et al., 1993a). In our case it yields a fit represented by the solid line in Fig. 3 *b* and a low effective frequency mode at 150 cm^{-1}. That is not unreasonable, given that some out-of plane porphyrin modes have been predicted to exist close to this frequency (Czernuszewicz et al., 1988).

Even though the 3b model is capable of reproducing our data, and despite the fact that the observed temperature dependence of the frequency of the central band can well be explained, we do not regard it as an appropriate model for the following reasons. Fig. 3 *c* shows the intensity ratios of the subbands as a function of temperature. It turns out that in particular the intensity ratio of the central and the 241 cm^{-1} band shows a totally unsystematic behavior. This scattering is significantly larger than would be expected from the statistics of the fits (maximum 30% variation) and gives no physical sense. Moreover, it is difficult to understand the broad halfwidths obtained for two of the bands. These would clearly be indicative of inhomogenous broadening. Comparison with other results and models (Šrajer et al, 1986; Šrajer and Champion, 1988; Champion, 1992) suggests that such an inhomogeneity would result from a distribution of multiple CSs. In this case, however, one would expect some temperature dependence of the halfwidths above the freezing temperature (Cupane et al., 1993a,b; Leone et al., 1994) in contrast to our findings. Finally, it should be mentioned that the $\nu_{Fe\text{-}His}$ bands of

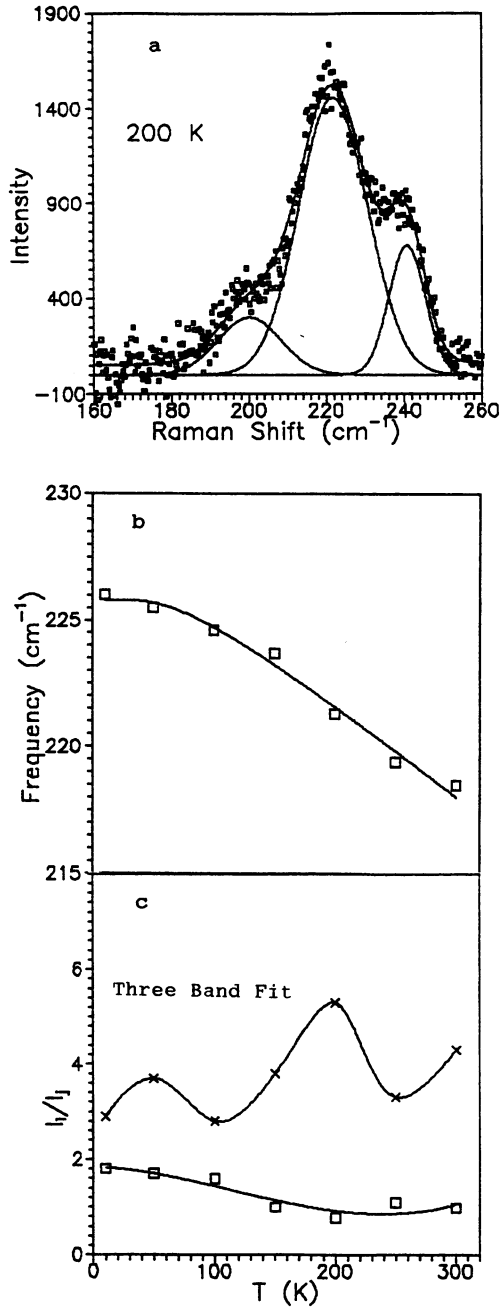

FIGURE 3 (*a*) Fit to the $\nu_{Fe\text{-}His}$ band measured at 200 K using three Gaussian bands. (*b*) Temperature dependence of the frequency of the central Gaussian band depicted in *a*. (*c*) Temperature dependence of the intensity ratios I_i/I_j of the bands i,j = 1,2,3 shown in *a*. The bands are ordered with respect to increasing frequencies; ×: $i = 2, j = 3$; □: $i = 1$, $j = 3$.

TABLE 1 χ_r^2 values of various fits for the $\nu_{Fe\text{-}His}$ band shapes shown in Fig. 1

T(K)	3b fit with three Gaussians	4b fit with four Gaussians	5b fits with four Lorentzians and one Gaussian
300	1.1	1.4	1.0
250	0.9	0.9	1.6
200	1.7	1.7	1.6
150	1.3	1.3	1.3
100	1.7	1.7	1.4
50	0.7	0.8	1.1
10	1.2	1.2	1.3

The effective numbers of free parameters used in these fits are nine, seven, and five for the 3b, 4b, and 5b model, respectively.

various hemoglobin derivatives and also some Mb mutants cannot sufficiently and consistently be described by such broad bands (Gilch et al., 1993). For instance, fits to the $\nu_{Fe\text{-}His}$ bands of the (sperm whale) Mb ($His^{E7} \rightarrow Gly$) and Mb($His^{E7} \rightarrow Met$) yield a decomposition into bands with halfwidths between 12 and 16 cm^{-1}. Corresponding band profiles of hemoglobin derivatives were found to be composed of bands with halfwidths between 10 and 13 cm^{-1}. The $\nu_{Fe\text{-}His}$ band of deoxyHb trout IV is significantly asymmetric and changes its shape as a function of pH. The minimal model that can consistently rationalize these data comprises five subbands with a common halfwidth of 12 cm^{-1}. A model based on an overlap of a few broad bands does not suffice (Bosenbeck et al., 1992).

In a second step we assumed that the overall band shape is composed of four Gaussian bands. In view of the results emerging from the fits with the 3b model we assumed that all halfwidths and the position of the band lowest in frequency do not depend on temperature. This reduced the effective number of free parameters from 12 to 7. Thus we obtained fits with χ_r^2 values between 0.7 and 1.7, indicating that, again, some fits reproduce features of the measured band shape that are statistically not significant. Fitting with Lorentzian profiles yields less convincing results. The temperature dependence of the intensity ratios of these bands as well as their frequencies exhibit some unsystematic scattering, while the halfwidths remain practically constant. No satisfactory fits are obtained (i.e., $\chi_r^2 > 2$) when the frequencies are assumed to be temperature independent. These observations lead us to the conclusion that a further modification of the model is required for an appropriate fitting of the entire data set.

In a final step we then utilized a model based on five bands (5b model) to fit our data. We now assumed that both frequencies and halfwidths of the bands are independent of temperature, thus reducing the effective number of free parameters to five. The apparent frequency shift of the overall band shape is now entirely considered as resulting from a redistribution of the intensities of the five bands. Such a model has earlier been successfully applied to rationalize the $T \rightarrow R$-induced frequency shift of the $\nu_{Fe\text{-}His}$ band in the spectra of deoxyHb derivatives (Gilch et al., 1993). The best fits were obtained by using a Gaussian profile for the band with the highest frequency and Lorentzian profiles for the remainder. This yields χ_r^2 values between 1 and 2 (cf. Table 1). Fig. 1 shows the fits to the $\nu_{Fe\text{-}His}$ band profiles measured at six different temperatures. The obtained frequencies of the underlying bands are 196, 209, 218, 226, and 240 cm^{-1}. The corresponding halfwidths are very similar (10–12.5 cm^{-1}) to those observed for Raman lines resulting from in-plane vibrations of the heme group (Gilch, 1994). The intensity ratios now show systematic temperature dependencies, which are depicted in Fig. 4, *a* and *b*. Interestingly, the intensity ratio of the bands observed at 198 and 240 cm^{-1} only slightly depend on temperature (Fig. 4 *b*, *lower curve*), while the relative intensities of the remaining bands exhibit a significant temperature dependence

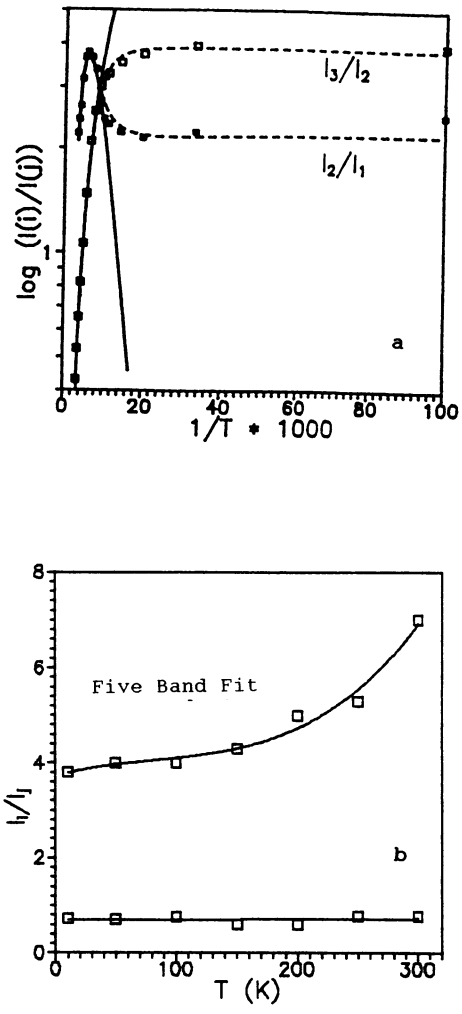

FIGURE 4 (*a*) Plot of the ratios of the $\nu_{Fe\text{-}His}$ subband intensities I_3/I_2 and I_2/I_1 versus reciprocal temperature. The solid lines represent fits carried out by employing the real temperature T in Eq. 9. These fits show good agreement with the experimental data in the temperature region between 300 and 150 K. Below 150 K it is necessary to introduce T_{eff} according to Eq. 4. The results are depicted by the dashed lines. (*b*) Plot of the intensity ratios $I(197)/I(240)$ (*lower curve*) and $(I_1 + I_2 + I_3)/I(240)$ (*upper curve*) versus temperature. The solid lines result from a linear and a spline fit to the data.

(Fig. 4 *a*). Hence, one suspects that the two bands at 198 and 240 cm^{-1} should not be attributed to the Fe-N_ϵ(His^{F8}) stretch. This is in accordance with Sassaroli et al. (1986), who assigned the shoulder on the high frequency side of the $\nu_{Fe\text{-}His}$ band to an out-of-plane pyrrole rocking mode of the heme macrocycle. In our analysis this shoulder is entirely accounted for by the band at 238 cm^{-1}. The origin of the low frequency line, which is absent in the corresponding spectrum of sperm whale Mb (Gilch et al., 1993), is unclear. The remaining bands obtained at $\Omega_1 = 209\ cm^{-1}$, $\Omega_2 = 218\ cm^{-1}$ and $\Omega_3 = 226\ cm^{-1}$ are now labeled as subbands Sb_1, Sb_2, and Sb_3 of the $\nu_{Fe\text{-}His}$ band, respectively. They are interpreted as resulting from different conformational substates of the Fe-His^{F8} linkage.

Fig. 4 *a* displays the intensity ratios I_3/I_2 and I_2/I_1 as a function of the inverse temperature. The ratio I_3/I_2 exhibits a van't Hoff behavior (*small dots*) between 300 and 150 K. Then the curves bend and the ratio stays constant for temperatures <70 K. The temperature dependence of the ratio I_2/I_1 is different. At room temperature a steep increase is observed, and a maximum arises at ~200 K. The ratio then decreases and becomes also constant below 70 K.

Interestingly, we also found that the intensity ratio calculated by dividing the total integrated intensity of the $\nu_{Fe\text{-}His}$ band (i.e., $I_1 + I_2 + I_3$) by the intensity of the 240 cm^{-1} band increases above ~150 K while it stays constants below. This suggests that the intrinsic Raman cross section of the $\nu_{Fe\text{-}His}$ mode is temperature dependent and reflects conformational changes along a coordinate different from those affecting the frequencies of its subbands (Friedman et al., 1990; Ahmed et al., 1991; Bosenbeck et al., 1992; Schweitzer-Stenner et al., 1993b).

We have carried out another experiment on the temperature dependence of the $\nu_{Fe\text{-}His}$ band, which yielded the same results when it was analyzed in terms of the above 5b model.

The spectral analysis of the $\nu_{Fe\text{-}His}$ was also performed with other band profiles. We found that fits with five Lorentzians and five Gaussians are significantly less successful than the above analysis based on four Lorentzians and one Gaussian profile. Successful fitting was obtained, however, by substituting the four Lorentzians by Voigtian profiles with a common Gaussian contribution of 8 cm^{-1}. This procedure yields intensity ratios of the subbands that are practically identical to those obtained from the fits with four Lorentzians and one Gaussian. Hence, each subband may still be inhomogenously broadened. That would be indicative of CS belonging to a higher tier of the conformational hierarchy.

DISCUSSION

In accordance with earlier results (Ahmed et al., 1991) the present data clearly show that the $\nu_{Fe\text{-}His}$ band deoxyMb exhibits a strong temperature dependence of both its apparent peak frequency and its band shape. It overlaps with two bands that most probably result from out-of-plane modes of the porphyrin macrocycle. We found that the minimal model to which all the $\nu_{Fe\text{-}His}$ bands recorded in this study could be fitted in a physically reasonable way comprises three Lorentzian subbands at $\Omega_1 = 209\ cm^{-1}$, $\Omega_2 = 218\ cm^{-1}$, and $\Omega_3 = 226\ cm^{-1}$ with halfwidths between 10.5 and 12 cm^{-1}. Both frequencies and halfwidths of the subbands were assumed to be temperature independent. These subbands are attributed to different CSs of the Fe-His^{F8}-linkage. Thus our interpretation of the $\nu_{Fe\text{-}His}$ band is in some regard different from other models, which assume a Gaussian distribution of the heme iron displacements reflecting a random distribution of CS in the protein environment of the heme (Šrajer et al., 1986, 1988; Šrajer and Champion, 1991; Cupane et al., 1993a,b). Our model rather points to some similarities between the proximal Fe-His^{F8} and the distal Fe-CO-His^{E7} (in MbCO) linkage. The latter also exhibits distinguishable CS as inferred from the subbands of the IR band arising from the stretching mode of the heme-bound CO (Ansari et al., 1987; Hong et al., 1990).

In the following we first analyze the temperature dependence of the intensity ratios of the above-derived $\nu_{Fe\text{-}His}$ subbands in terms of a thermodynamic model. Thereafter we discuss some of the physical consequences to be drawn from the results of our analysis. We then compare our interpretation with a possible alternative model emerging from most recent studies on the relaxation dynamics of MbCO*. Finally we discuss some structural aspects of our result.

Temperature dependence of $\nu_{Fe\text{-}His}$

We assume that each subband is related to a distinct CS. As long as these are in thermodynamic equilibrium their intensity ratios are given by:

$$I_i/I_j = \sigma_i/\sigma_j \exp(\Delta S_{ij}/R) \exp(-\Delta H_{ij}/RT)$$
$$= A_{ij} \exp(-\Delta H_{ij}/RT) \quad (3)$$

R is the universal gas constant, ΔS_{ij} is the entropic and ΔH_{ij} the enthalpic difference between the CS i and j. σ_i and σ_j denote the Raman scattering cross sections, which might differ for different CSs because of their dependence on the geometric parameters of the Fe-His^{F8} complex (Ahmed et al., 1991; Bosenbeck et al., 1992; Gilch et al., 1993; Stavrov, 1993). In the following we assume that σ_i/σ_j does not depend on temperature.

Eq. 3 is valid in the high temperature regime in which thermal fluctuations across the barriers between the CS are possible and the thermodynamic equilibrium is therefore maintained. This is reflected by a van't Hoff behavior of the corresponding intensity ratios. At low temperatures, however, a gradual freezing of the substates population results on the experimental time scale and finally the population of the distinct CS freezes completely and stays independent of temperature. As shown in Fig. 4 *a*, this is observed for both intensity ratios of the $\nu_{Fe\text{-}His}$.

To quantify more exactly the freezing temperature and the transition region, we introduce a heuristic effective temperature T_{eff} with the property that at high temperatures where equilibrium is maintained T_{eff} equals the actual temperature T. Well below the freezing point the ratio of the populations of two distinct substates is determined by a temperature T_f at which freezing has been established. Therefore the effective temperature has to approach T_f below T_f. In the intermediate region ΔT the effective temperature deviates from the actual temperature due to incomplete equilibration. A function with such properties is given by:

$$T_{eff} = \frac{T_f}{1 + \exp((T - T_f)/\Delta T)} + \frac{T}{1 + \exp((T_f - T)/\Delta T)} \quad (4)$$

where ΔT is the width of the transition region. T_f and ΔT can be dependent of the conversion pair CS_i and CS_j, if the barriers separating different pairs are not identical.

Introducing T_{eff} for T into Eq. 3 yields an expression that can well be fitted to the temperature dependence of I_3/I_2, but at high temperatures deviations from the experimental data are observed. The maximum in the ratio I_2/I_1, however, cannot be reproduced by Eqs. 3 and 4. Similar maxima or minima were earlier observed by Hong et al. (1990) in the intensity ratios of the subbands A_0 and A_1 of the IR band resulting from the CO stretch of MbCO. To explain these features the authors noted that the specific heat c_p of proteins depends linearly on temperature between 40 and 320 K (Mrevlishvili, 1979). In this case the following expression for the entropy is obtained:

$$S(T) = \int \frac{c_p(T)}{T} \cdot dT = a + c_p(0) \ln(T/T_0) + bT \quad (5)$$

$$c_p(T) = c_p(0) + bT \quad (6)$$

The experimental $c_p(T)$ data (Mrevlishvili, 1979) show that the term $a + c_p(0) \ln(T/T_o)$ remains constant within <10% between 100 and 300 K. Therefore, $S(T)$ can be written as:

$$S(T) = S(0) + bT \quad (7)$$

From the thermodynamic relation $(\partial H/\partial T)_p = T\,(\partial S/\partial T)_p$ we obtain:

$$H(T) = H(0) + 1/2bT^2 \quad (8)$$

Introducing Eqs. 7 and 8 into Eq. 3 and further replacing T in Eq. 3 by T_{eff} of Eq. 4 we obtain:

$$I_i/I_j = A_{ij} \exp(-(\Delta H_{ij}(0)/RT_{eff}) + b_{ij}T_{eff}/2R) \quad (9)$$

where

$$A_{ij} = \sigma_i/\sigma_j \exp(\Delta S_{ij}(0)/R)$$

b_{ij} is the difference between the slope of $c_p(T)$ in the substates j and i and gives the first derivative of the entropy with respect to the temperature. Eq. 9 differs from Eq. 3 by this term, which gives rise to the maxima and minima of I_i/I_j. Fitting Eq. 8 to I_2/I_1 yields excellent agreement with the experimental data, as judged by the dashed line in Fig. 4 *a*. Since a linear dependence of $c_p(T)$ is expected for all CSs, we have also used Eq. 9 to fit the ratio I_3/I_2, thus yielding again good agreement with the experimental data (Fig. 4 *a*). The parameters obtained from both fits are listed in Table 2.

Globular proteins have b values in the range of 70 J/mol K^2 (Mrevlishvili, 1979). Thus the above data indicate to changes in b of about 0.5% when switching from one substate into another. This seems to be reasonably small. It should be noted that the existence of a maximum in the temperature dependence of I_i/I_j is a necessary consequence of a linear temperature dependence of the difference in specific heat between two distinct CSs. If this difference is as small as it seems to be between CS_2 and CS_3 the maximum is shifted to higher temperatures and may not be observable because heme proteins denaturate at about 330 K.

If we assume $\sigma_1 = \sigma_2$ for the Raman cross section we can estimate the entropy change ΔS_{21} between CS_1 and CS_2 to 40 J/K. The total entropy of globular proteins at room temperature has been estimated from their specific heat to S (298 K) $\approx$ 10 kJ/K (Mrevlishvili, 1979). Thus the transition $CS_2 \rightarrow CS_1$ brings about an entropic change of 0.1% of the total entropy of the protein. The enthalpic difference between CS_2 and CS_1 of 2.8 kJ/mol is also small compared with the difference in the enthalpy of the protein between $T = 0$ and room temperature, which is in the order of 3000 kJ/mol. A similar result emerges for CS_2 and CS_3.

Temperature dependence of the IR band resulting from the CO stretch in MbCO

Another spectral marker, i.e., the IR band resulting from the stretching mode of the heme-bound CO, has extensively been utilized to study conformational substates in sperm whale MbCO. Ansari et al. (1987) have shown that this band can be decomposed into three Voigtian subbands denoted as A_0, A_1 and A_3. The intensity ratios A_0/A_1 and A_1/A_3 show a temperature dependence that in many respects parallels that of the $\nu_{Fe\text{-}His}$ subbands (Ansari et al., 1987; Iben et al., 1989; Hong et al., 1990). Fig. 5 displays the

TABLE 2 Thermodynamic parameters derived from the temperature dependence of the $\nu_{Fe\text{-}His}$ sublines' intensity ratios

Intensity ratios	ΔH_{ij} (kJ/mol)	ΔS_{ij} (J/mol K)	b_{ij} (J/mol K)	T_f (K)	ΔT (K)
I_2/I_1	2.8	44	−0.16	117	55
I_3/I_2	−0.5	15	−0.16	117	55

The standard deviations have been estimated to be 10% for ΔH_{ij} and ΔS_{ij} and ±5 K for T_f and ΔT.

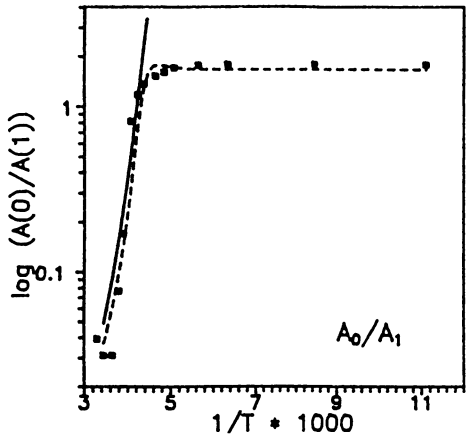

FIGURE 5 Plot of total absorption ratios exhibited by the subbands A_0 and A_1 of the (Mb)COS IR band versus reciprocal temperature (data taken from Ansari et al., 1987). The solid line represents a fit with real temperature T, while the dashed line displays a fit for which the effective temperature T_{eff} is used.

temperature dependence of A_0/A_1 of MbCO in an aqueous solution as reported by Ansari et al. (1987). It deviates from a van't Hoff behavior at temperatures above 250 K and below 230 K. The dashed line results from a fit of Eq. 9 to these data. The parameters are listed in Table 3.

Assuming that the absorption cross sections of the CO stretch are identical in both CSs (Ormos et al., 1988), we obtain $\Delta S_{01}{}^{CO} \approx 490$ J/K. This is larger by more than an order of magnitude in comparison with the entropic change obtained for the Fe-His^{F8} CS in horse heart deoxy Mb. The parameter $b_{01}{}^{CO}$ is also by one order of magnitude larger compared with the b_{21} values of the Fe-His^{F8} CS.

Whereas freezing of the Fe-His^{F8} CSs occurs in a wide range ($\Delta T = 55$ K) around the freezing temperature $T_f = 117$ K, the CS monitored by the CO stretch in sperm whale MbCO freeze out in an extremely narrow range of $\Delta T = 8$ K at $T_f = 231$ K. This finding is of particular interest, because it suggests that the freezing behavior of the sperm whale MbCO substates resembles that of protein-bound water, which occurs between 190 and 250 K at high degrees of hydration (Doster et al., 1986). Goldanskii and Krupyanskii (1989) show that crystals of met-Mb and also samples with hydration degrees of about 1.5 g H_2O/g protein exhibit a freezing of their hydration shell at ~260 K with a narrow transition region of $\Delta T = 3 \pm 1$ K.

From the temperature dependence of protein-bound water (Goldanskii and Krupyanskii, 1989) we estimate $b \approx 0.6$ J/mol K^2. Given that the protein at high degrees of hydration carries bound water of about half its weight, the hydration shell contains about 350 H_2O molecules (Steinbach and Brooks, 1993). Thus the value b_H for the hydration shell amounts to 200 J/mol K^2 in accordance with recent data from Miyazaki et al. (1993). Thus the corresponding change of $b_{CO} = 3.5$ J/mol K^2 derived from the above MbCO data seems to be reasonably small. Therefore we are led to the conclusion that the thermal fluctuations between the CSs monitored by the CO stretch in sperm whale MbCO are driven by fluctuations of protein bound water. It is noteworthy in this context that in ethylene glycol buffer and in pure glycerol solution of sperm whale MbCO the A_0/A_1 ratio deviates from the van't Hoff behavior at much lower temperatures (180 K) and exhibit a broader transition region reflecting again the properties of the solvent, i.e., the glass transition of glycerol. Moreover the A_0/A_1 ratio exhibit extrema at high temperatures, which can also be reproduced by Eq. 9 with fitting parameters comparable to ours (Hong et al., 1990).

TABLE 3 Thermodynamic parameters derived from the temperature dependence of the A_0/A_1 ratio obtained from the IR band of the COS in sperm whale MbCO (Ansari et al., 1987)

	ΔH_{ij} (kJ/mol)	ΔS_{ij} (J/mol K)	b_{ij} (J/mol K)	T_f (K)	ΔT (K)
A_0/A_1	−79	−490	1.35	231	8

The standard deviations have been estimated to be 10% for ΔH_{ij} and ΔS_{ij}, ±5 K for T_f and ±2 for ΔT.

In view of these considerations we interpret the freezing of the Fe-His^{F8} substates as reflecting internal processes in the heme environment that are not significantly coupled to the hydration shell. That notion is corroborated by earlier spectroscopic studies on hydrated Mb and hemoglobin films. Brown et al. (1983) found that the intensity ratio of the CO stretch sublines in sperm whale MbCO and HbCO change drastically upon dehydration of the films giving rise to a more open distal pocket configuration. These changes are completely reversible. These results suggest that the constraints by the hydration shell exert significant influence to the distal side of both proteins. Furthermore, the $\nu_{Fe\text{-}His}$ band of the transient HbCO* species obtained at 10 ns after photolysis was found to be unaffected by hydration (Findsen et al., 1986). This seems to indicate that at least in deligated heme proteins the Fe-His^{F8} linkage band is not responsive to interactions between the hydration shell and the protein, in accordance with our results.

In this context some results reported by Cupane et al. (1993a,b) are noteworthy. These authors carefully measured the temperature dependence of the Soret band in the optical spectra of deoxyMb and MbCO for sperm whale, horse heart, and elephant Mb. They analyzed the band shape of the Soret band by invoking Franck Condon transitions of several high and low frequency modes into the excited B-state of the porphyrin macrocycle. The contributions from a bath of low frequency modes were accounted for by a Gaussian distribution of width σ, which was obtained from a fit to Soret bands measured at different temperatures between 10 and 300 K. If the low frequency vibrations are harmonic, σ should exhibit a temperature dependence that can be described by an equation of the type $\sigma^2 \sim \coth(h\nu/2kT)$, where ν is regarded as an effective frequency representing the entire bath of low frequency modes. Deviations from this behavior indicate that these modes have become anharmonic, because they now involve structural fluctuations between different CS in the protein environment of the

heme. All CO-ligated Mbs investigated show such deviations above 180 K. This temperature is close to the glass transition of the glycerol water mixture in which the proteins were dissolved. For the corresponding deoxyMbs, however, an onset of anharmonic motions was already observed at 110 K. In accordance with our data this finding suggests that deoxyMb exhibits thermal fluctuations within its heme environment, which are not induced by protein-solvent interactions. Most recent investigations of the Soret band's thermal broadening in model heme complexes have provided strong evidence that the coupling of these thermal motions to the electronic transitions of the heme depends critically on the position of the heme iron (Leone et al., 1994).

It should be emphasized that the above results are unexpected. Crystallographic studies (Frauenfelder et al., 1979), neutron scattering (Doster et al., 1989), and Mössbauer experiments (Parak et al., 1982) show an onset of anharmonic, thermal motions between CSs of Mb occurring above 200 K. The discrepancy between our data and the results from Mössbauer experiments is of particular importance, because the latter monitors the mean square displacement of the heme iron. Parak et al. (1982) have shown that the latter increases above 200 K. This coincides with the onset of fluctuations in the crystal water and suggests that the iron motion is governed by interactions between the protein and water molecules of its hydration shell. This notion is supported by the observation that the iron motion is still harmonic even at 300 K if the experiment is carried out with frozen, dry proteins (Parak, 1986). This discrepancy between the temperature dependence of Mössbauer and $\nu_{\text{Fe-His}}$-data is dealt with below, as we discuss the structural interpretation of our data.

As already shown by Ansari et al. (1987), a decrease in pH also causes the A_0/A_1 ratio to increase (cf. also Morikis et al., 1989). One may therefore suspect that the A_0/A_1 increase with decreasing temperature results from the protonation of neutral and acid amino acid residues, which could become protonated by an increase in their pK values (Braunstein et al., 1993) and/or by a decrease in the pH of the solvent. Indeed, Astl and Mayer (1991) have shown that the sodium phosphate buffer used in the study of Ansari et al. (1987) jumps to lower pH upon crystallization of bulk water. However, if protonation processes would be the main cause for the observed changes in A_0/A_1 and the intensity ratios of the $\nu_{\text{Fe-His}}$, one would expect an S-shaped titration curve rather than a linear van't Hoff behavior above the freezing temperature. This has not been observed. Moreover, the freezing of bulk water can be expected to significantly decrease the proton conductivity, so that protonation processes become unlikely. Finally, we have used potassium phosphate buffer in the present study on the $\nu_{\text{Fe-His}}$ band, which due to Astl and Mayer (1991) does not show a temperature jump upon water crystallization. Hence, we can rule out that any temperature dependence of the intensity ratios discussed in this study results from protonation processes.

Comparison with other experiments

It has been pointed out to us that, instead of invoking a lower freezing temperature, our data may well be explained by assuming light-driven relaxation processes to be operative between 200 and 100 K. (H. Frauenfelder, G. U. Nienhaus, J. M. Friedman, personal communications). Such processes have most recently been established for photodissociated MbCO* at temperatures between 80 and 180 K (Chu et al., 1995; Nienhaus et al., 1994). These authors observed that in the photolyzed MbCO* the effective barrier for CO rebinding in the heme pocket is shifted from its position to higher values upon constant and comparatively intensive irradiation of the sample. By inspection of the IR band resulting from the vibration of the unbound CO the authors ruled out that this process involves a conformational change in the protein environment of the photodissociated ligand as it was earlier proposed by Powers et al. (1987) and Šrajer et al. (1991). The phenomenon most likely results from conformational changes within the Fe-His complex, the geometry of which is known to determine the rate both of association and dissociation of the ligand (Friedman, 1985; Schweitzer-Stenner, 1989; Steinbach et al., 1991; Schweitzer-Stenner and Dreybrodt, 1992). Such light-induced structural variations may become possible even below the freezing temperature, if the excited electronic states of the heme populated by photon absorption exhibit significantly lower barriers between the CSs. In this case conformational fluctuations can occur on a time scale comparable with the lifetime of this state, and photon absorption may cause a rearrangement of non-equilibrium CS distributions. Consequently it may also affect the temperature dependence of the $\nu_{\text{Fe-His}}$ band. Indeed it was already shown by Ahmed et al. (1991) that the $\nu_{\text{Fe-His}}$ band of the photolyzed MbCO* is responsive to optical pumping below 100 K.

Even though we find this idea very fascinating, we have to rule out its applicability to the present data, because optical pumping would result in some type of hysteresis effect, i.e., we should observe different spectra for the cooling and warming up periods of our experiment. As already stated in the "Results" section this was not observed. However, it would be of extraordinary interest to check whether optical pumping can occur also in the pure deoxy state of Mb.

Recently, Rosenfeld and Stavrov (1994) have rationalized the temperature dependence of the $\nu_{\text{Fe-His}}$ band profile by invoking anharmonic coupling between Fe-N_ϵ(His ^{F8}) stretch and a heme doming mode with an estimated frequency of 50 cm^{-1}.The model also yields sublines of the $\nu_{\text{Fe-His}}$ band, which result from Raman scattering involving $1 \rightarrow 2$, $2 \rightarrow 3$, $3 \rightarrow 4$, etc., transitions due to the thermal population of higher vibrational states. The corresponding frequencies are different because of anharmonicity of the ground state potential. In view of this prediction one would suspect that our subbands could result from such an interaction rather than from CS. However, the model of Rosen-

feld and Stavrov predicts significant narrowing of the overall band shape with decreasing temperature. This has not been observed in our experiment (cf., the above discussion of the 3b analysis). Moreover, one would expect an asymmetric $\nu_{\text{Fe-His}}$ band shape at room temperature and a symmetric one at 10 K. This also is not in accordance with the results of our 5b analysis.

Structural aspects

In our earlier study (Schweitzer-Stenner et al., 1993b; Gilch et al., 1993) we combined models proposed by Friedman et al. (1990) and Stavrov (1993) in that we assigned different $\nu_{\text{Fe-His}}$ subbands to CSs that exhibit different tilt angles and out of plane displacements of the iron in the heme. Because it is expected (Stavrov, 1993) that an increase of the Fe displacement brings about an decrease of the $\nu_{\text{Fe-His}}$ frequency the present data indicate a situation in which a CS with lower Fe displacement is more populated at lower temperature.

Most recently Della Longa et al. (1994) have reported the results of x-ray absorption near edge structure (XANES) spectroscopy on the photoproducts of MbCO at temperatures below 50 K. They have interpreted their results as indicative of the existence of at least two CSs differing in terms of heme doming and Fe out-of-plane displacement. Our results are obtained from pure deoxyMb species so that they are not directly comparable with the XANES data. However, the latter show that a model based on spectroscopically distinguishable CS of the Fe-His^{F8} linkage rather than on unresolvable (Gaussian) distributions is supported by other experimental data.

In this context it is necessary to address the contradiction between the Mössbauer data and the behavior of the $\nu_{\text{Fe-His}}$ band. At room temperature the Fe motion monitored by the Mössbauer experiment involves a length of nearly 0.3 Å (Parak et al., 1982), which is in the order of magnitude of the Fe displacement in Mb (Phillips, 1981). To estimate the possible difference between the Fe displacements reflected by the $\nu_{\text{Fe-His}}$ subbands we utilize an empirical equation that was derived by Stavrov (1993) from an analysis of the $\nu_{\text{Fe-His}}$ band of porphyrin-imidazole compounds:

$$\Omega_j = 209.4\ \text{cm}^{-1} - 184\ \text{cm}^{-1}/\text{Å}[\delta_j - 0.4\ \text{Å}] \quad (10)$$

where Ω_j is the frequency of the jth subband and δ_j denotes the corresponding Fe displacement. Inverting Eq. 9 and inserting the frequencies of the three observed $\nu_{\text{Fe-His}}$ subbands yields $\delta_1 = 0.40$ Å, $\delta_2 = 0.35$ Å, and $\delta_1 = 0.31$ Å. Thus we obtain ~0.09 Å difference between the maximal and minimal Fe displacement, which is by a factor of 3.3 smaller than the length of the Fe motion inferred from the Mössbauer data. This points to the different character of the motions probed by the above experiments. While the Raman data and also the optical absorption data reported by Cupane and co-workers (Cupane et al., 1993a,b) are sensitive to such Fe motions that alter the Fe-heme plane distance, the Fe motions detected by the Mössbauer data most probably involve the entire heme. Hence, the Fe displacement remains unaffected.

In an earlier study Sassaroli et al. (1986) rationalized the temperature dependence of the frequency of the $\nu_{\text{Fe-His}}$ band shape in terms of the decrease of the Fe^{2+}-mean square displacement with decreasing temperature as inferred from the Mössbauer data of Parak and associates (1982). The differences between the temperature dependence of Mössbauer and Raman data revealed by our experiment contradict this explanation.

The above considerations led us to the conclusion that the thermal fluctuations above 120 K monitored by the $\nu_{\text{Fe-His}}$ and the optical absorption band (Cupane et al., 1993a,b) involve CS, which should be assigned to a higher tier in the conformational hierarchy than the motions probed by Mössbauer experiments. We propose that the fluctuations between the Fe-His^{F8} substates arise from conformational changes that involve torsional motions of some protein side chains located in the F and FG helices. Molecular dynamics calculations on Mb have indeed indicated that some of the amino acid residues may start to exhibit torsional motions above 100 K (Loncharich and Brooks, 1990). The Fe motions inferred from the Mössbauer experiment, however, may be induced by heme-protein coupling, which imposes the motion of larger protein segments on the entire heme group. A theoretical analysis of the Mössbauer data by Knapp et al. (1983) suggested that the iron is coupled to three types of protein motions. Two of them can be described as overdamped Brownian oscillators, while the third was interpreted as free diffusional motion of protein segments within the time scale of the experiment.

In this context it is noteworthy that β-relaxation in polymers proceeds on a faster time scale and exhibits lower freezing temperatures than α-relaxation processes (Green et al., 1994). The characteristic times of β-relaxations normally obey an Arrhenius law, although their time course is significantly non-exponential (Götze and Sjörgen, 1992). In polymers these relaxations are determined by the side chain structure. Hence, one may suppose that the present $\nu_{\text{Fe-His}}$ reflect CSs, the fluctuations between which are connected to β-relaxation processes owing to the fluctuation-dissipation theorem. This hypothesis is to some extent supported by the broad transition region of $\Delta T = 55$ K, which may be indicative of a more Arrhenius-like character of the involved effective relaxation times.

At present we cannot give a final explanation for the different behavior of MbCO and deoxyMb. One may speculate that in MbCO the electronic transitions of the heme group are decoupled from such protein motions affecting the Fe displacement (Champion, 1992; Leone et al., 1994), because porphyrin and iron orbitals do not overlap in the case of an in-plane configuration of the metal (Zerner et al., 1966; Stavrov, 1993). On the other hand the CO ligand may couple the heme to protein motions at its distal side. Protein motions are known to proceed on a slower time scale than are proximal motions (Tian et al., 1992; Champion, 1992).

Further investigations are necessary to clarify this important issue.

SUMMARY

The $\nu_{Fe\text{-}His}$ Raman band of horse heart deoxyMb is composed of three subbands at $\Omega_1 = 209\ cm^{-1}$ (Sb_1), $\Omega_2 = 218\ cm^{-1}$ (Sb_2), and $\Omega_3 = 226\ cm^{-1}$ (Sb_3). Their intensities are significantly temperature dependent between 300 and 80 K. These subbands are attributed to different conformational substates of the Fe-His^{F8} linkage. A thermodynamical model was utilized to fit the temperature dependence of the intensity ratios I_2/I_1 and I_3/I_2. It is based on a modified van't Hoff equation accounting for the freezing of the protein into a non-equilibrium distribution of its conformational substates below a temperature T_f and for the linear dependence of the specific heat c_p. This yields a freezing temperature of $T_f = 117$ K and a rather broad transition region of $\Delta T = 55$ K. By revisiting the temperature dependence of the subbands of the IR band resulting from the COs in sperm whale MbCO, we found that the corresponding conformational substates are frozen at a much higher temperature, i.e., $T_f = 231$ K. This value and the comparatively small width of the transition region ($\Delta T = 8$ K) suggest that the fluctuations between these conformational substates are strongly coupled to protein-bound water. In contrast the conformational substates inferred from the $\nu_{Fe\text{-}His}$ band reflect intrinsic properties of protein segments in close proximity to the heme group. They most probably belong to a higher tier in the hierarchy of conformational substates.

Note added in proof—Just after this paper had been accepted, a paper by Sage et al. (1995) came to our attention. It reports a detailed study on the influence of temperature and solvent on the $\nu_{Fe\text{-}His}$ band of sperm whale Mb in its deoxygenated and photolyzed (MbCO*) state. The authors claim that a single Lorentzian band is sufficient to describe the $\nu_{Fe\text{-}His}$ band. The temperature dependence of its peak frequency is rationalized in terms of anharmonic coupling similar to our interpretation of the results of our 3b analysis. Further experiments are of course necessary to finally decide which interpretation is the correct one. We like to emphasize, however, that the $\nu_{Fe\text{-}His}$ bands of horse heart and sperm whale Mb are somewhat different. The Raman band of the latter is less broadened and its subband spectrum indicates much lower intensities of Sb_1 and Sb_2 compared with those of horse heart Mb. It is likely that this reflects differences in the heterogeneity of the proximal environment. This and some further results emerging from the study of Sage et al. (1995) clearly demonstrate the structural sensitivity of the $\nu_{Fe\text{-}His}$ band, which we believe is also an appropriate basis for understanding its temperature dependence.

We are indebted to Hans Frauenfelder and G. Ulrich Nienhaus for bringing to our attention their recent work on optical pumping effects in Mb, for helpful discussions, and for providing us their manuscripts before publication. We wish to thank Joel M. Friedman for valuable discussions, Peter Steinbach for providing us information about his molecular dynamics calculations on an Mb-water system, and Gerald Kirchner for critically reading the manuscript and for helpful discussions on the application of χ^2 tests.

This paper was written in part when R.S.S. was a Max Kade fellow with Dr. Samuel Krimm at the Biophysics Research Division of the University of Michigan, Ann Arbor.

REFERENCES

Ahmed, A. M., B. F. Campbell, D. Caruso, M. R. Chance, M. D. Chavez, S. H. Courtney, J. M. Friedman, I. E. T. Iben, M. R. Ondrias, and M. Yang. 1991. Evidence for proximal control of ligand specificity in heme proteins: absorption and Raman studies of cyrogenically trapped photoproducts of ligand bound myoglobin. *Chem. Phys.* 158:239–351.

Ansari, A., J. Berendzen, S. F. Browne, H. Frauenfelder, I. E. T. Iben, T. B. Sauke, E. Shysamunder, and R. D. Young. 1985. Protein states and protein quakes. *Proc. Natl. Acad. Sci. USA.* 82:5000–5004.

Ansari, A., J. Berendzen, D. Braunstein, B. R. Cowen, H. Frauenfelder, M. K. Kong, I. E. T. Iben, J. B. Johnson, P. Ormos, T. B. Sauke, R. Scholl, A. Schulte, P. J. Steinbach, J. Vittitow, and R. D. Young. 1987. Rebinding and relaxation in the heme pocket. *Biophys. Chem.* 26:337–355.

Antonini, E., and M. Brunori. 1970. Hemoglobin and Myoglobin in Their Reaction with Ligands. Elsevier, Amsterdam.

Asher, S. A., and J. Murtaugh. 1983. Metalloporphyrin gas and condensed-phase resonance Raman studies: the role of vibrational anharmonicites as determinants of Raman frequencies. *J. Am. Chem. Soc.* 105: 7244–7251.

Astl, G., and E. Mayer. 1991. Alkali cation effect on carbonylhemoglobin's and myoglobin's conformer populations when exposed to freeze-concentration of their phosphate-buffered aqueous solutions. *Biochim. Biophys. Acta.* 1080:155–159.

Austin, R. H., and C. M. Chen. 1992. The spin-glass analogy in protein dynamics. *In:* Spin Glasses and Biology. D. L. Stein, editor. World Scientific, Singapore. 179–223.

Austin, R., K. W. Beeson, L. Eisenstein, H. Frauenfelder, and I. C. Gunsalus. 1975. Dynamics of ligand binding to myoglobin. *Biochemistry.* 14:5355–5373.

Bevington, P. R. 1969. Data Reduction and Error Analysis for the Physical Science. McGraw-Hill, New York.

Bosenbeck, M., R. Schweitzer-Stenner, and W. Dreybrodt. 1992. pH-induced conformational changes of Fe^{2+}-N_ϵ(His F8) linkage in deoxyhemoglobin trout IV detected by the Raman active Fe^{2+}-N_ϵ(His F8) stretching mode. *Biophys. J.* 61:31–41.

Braunstein, D. P., K. Chu, K. D. Egeberg, H. Frauenfelder, J. R. Mourant, G. U. Nienhaus, P. Ormos, S. G. Sligar, B. A. Springer, and R. D. Young. 1993. Ligand binding to heme proteins. III: FTIR Studies of His-E7 and Val-E11 mutants of carbonmonoxymyoglobin. *Biophys. J.* 65:2447–2454.

Brown, W. E., J. W. Sutcliffe, and P. D. Pulsinelli. 1983. Multiple internal reflectance infrared spectra of variably hydrated hemoglobin and myoglobin films: effects of globin hydration on ligand conformer dynamics and reactivity at the heme. *Biochemistry.* 22:2914–2923.

Campbell, B. F., M.. R. Chance, and J. M. Friedman. 1987. Linkage of functional and structural heterogenity in proteins: dynamic hole burning in carbonmonoxymyoglobin. *Science (Washington D.C.).* 238:373–376.

Champion, P. M. 1992. Raman and kinetic studies of myoglobin structure and dynamics. *J. Raman Spectrosc.* 23:557–567.

Chavez, M. D., S. H. Courtney, M. R. Chance, D. Kiula, J. Nocek, B. M. Hofman, J. M. Friedman, and M. R. Ondrias. 1990. Structural and functional significance of inhomogenous line broadening of band III in hemoglobin and Fe-Mn hybrid hemoglobin. *Biochemistry.* 29: 4844–4852.

Chu, K., R. M. Ernst, H. Frauenfelder, J. R. Mourant, G. U. Nienhaus, and R. Phillipp. 1995. Light-induced and thermal relaxation in a protein. *Phys. Rev. Lett.* 74:2607–2610.

Cupane, A., M. Leone, and E. Vitrano. 1993a. Protein dynamics: conformational disorder, vibrational coupling and anharmonicity in deoxyhemoglobin and myoglobin. *E. Biophys. J.* 21:385–391.

Cupane, A., M. Leone, E. Vitrano, L. Cordone, U. R. Hitpold, K. H. Winterhalter, W. Yu, and E. E. Di Iorio. 1993b. Structure-dynamics-function relationships in Asian elephant (*Elephas maximus*) myoglobin. An optical spectroscopy and flash photolysis study on functionally important motions. *Biophys. J.* 65:2461–2472.

Czernuszewicz, R. S., X.-Y. Li, and T. G. Spiro. 1988. Nickel octaethylporphyrin ruffling dynamics from resonance Raman spectroscopy. *J. Am. Chem. Soc.* 111:7024–7031.

Della Longa, S., I. Ascone, A. Fontaine, A. Congiu Castellano, and A. Bianconi. 1994. Intermediate states in ligand photodissociation of car-

boxymyoglobin studied by dispersive x-ray absorption. *E. Biophys. J.* 23:361–368.

Doster, W., D. Beece, S. F. Bowne, E. E. Di Iorio, L. Eisenstein, H. Frauenfelder, L. Reinisch, E. Shyamsunder, K. H. Winterhalter, and K. T. Yue. 1982. Control and pH-dependence of ligand binding to heme proteins. *Biochemistry.* 21:4831–4839.

Doster, W., A. Bachleitner, R. Dunau, M. Hiebl, and E. Lüscher. 1986. Thermal properties of water in myoglobin crystals and solutions at subzero temperatures. *Biophys. J.* 50:213–219.

Doster, W., S. Cusack, and W. Petry. 1989. Dynamic transition of myoglobin revealed by inelastic neutron scattering. *Nature (Lond.).* 337: 754–756.

Eaton, W. A., L. K. Hanson, P. J. Stephens, J. C. Sutherland, and J. B. R. Dunn. 1978. Optical spectra of oxy- and deoxyhemoglobin. *J. Am. Chem. Soc.* 100:4991–5001.

Findsen, E. W., P. Simons, and M. R. Ondrias. 1986. Response of the local heme environment of (carbonmonoxy) hemoglobin to protein dehydration. *Biochemistry.* 25:7912–7917.

Frauenfelder, H., and E. Gratton. 1986. Protein dynamics and hydration. *Methods Enzymol.* 127:207–216.

Frauenfelder, H., F. Parak, and R. D. Young. 1988. Conformational substates in proteins. *Annu. Rev. Biophys. Biophys. Chem.* 17:451–479.

Frauenfelder, H., G. A. Petsko, and D. Tsernoglou. 1979. Temperature dependent x-ray diffraction as a probe of protein structural dynamics. *Nature (London).* 280:558–563.

Frauenfelder, H., N. A. Alberding, A. Ansari, D. Braunstein, B. R. Cowen, M. K. Kong, I. E. T. Iben, J. B. Johnson, S. Luck, M. C. Marden, J. R. Mourant, P. Ormos, L. Reinish, R. Scholl, A. Schulte, E. Shysamunder, L. B. Sorensen, P. J. Steinbach, A.-H. Xie, R. R. Young, and K. T. Yue. 1990. Proteins and pressure. *J. Phys. Chem.* 94:1024–1037.

Friedman, J. M. 1985. Structure, dynamics and reactivity in hemoglobin. *Science (Washington D.C.).* 228:1274–1280.

Friedman, J. M., B. F. Campbell, and R. W. Noble. 1990. A possible new control mechanism suggested by resonance Raman spectra from a deep ocean fish hemoglobin. *Biophys. Chem.* 37:43–59.

Gilch, H. 1994. Ramanspektroskopische Untersuchungen an Myoglobin und Hämoglobin: Konformationssubzustände der Fe^{2+}-N_ϵ(His F8) Bindung. Doktorarbeit, Universität Bremen.

Gilch, H., R. Schweitzer-Stenner, and W. Dreybrodt. 1993. Structural heterogenity of the Fe^{2+}-Ne(His^{F8}) bond in various hemoglobin and myoglobin derivatives probed by the Raman-active iron histidine stretching mode. *Biophys. J.* 65:1470–1485.

Goldanskii, V. I., and Y. F. Krupyanskii. 1989. Protein and protein-bound water dynamics studied by Rayleigh scattering of Mössbauer radiation (RSMR). *Q. Rev. Biophys.* 22:39–92.

Götze, W., and L. Sjörgen. 1992. Relaxation processes in supercooled liquids. *Rep. Prog. Phys.* 55:241–376.

Green, J. L., J. Fan, and C. A. Angell. 1994. The protein-glass analogy: some insights from homopeptide comparisons. *J. Phys. Chem.* 98: 13780–13790.

Grinvald, A., and I. Z. Steinberg. 1974. On the analysis of fluorescence decay kinetics by the method of least square. *Ann. Biochem.* 59: 583–598.

Hays, W. L., and Winkler, R. L. 1970. Statistics. Probability, Inference and Decision, Vol. I. Holt, Rinehardt and Winston, New York.

Hong, M. K., D. Braunstein, B. R. Cowen, H. Frauenfelder, I. E. T. Iben, J. R. Mourant, P. Ormos, R. Scholl, A. Schulte, P. J. Steinbach, A.-H. Xie, and R. D. Young. 1990. Conformational substates and motions in myoglobin. External influences on structure and dynamics. *Biophys. J.* 58:429–436.

Iben, I. E. T., D. Braunstein, W. Doster, H. Frauenfelder, H. K. Kong, J. B. Johnson, S. Luck, P. Ormos, A. Schulte, P. Steinbach, A. Xie, and R. D. Young. 1989. Glassy behaviour of a protein. *Phys. Rev. Lett.* 62: 1916–1919.

Ivanov, D., J. T. Sage, M. Klein, J. R. Powell, S. A. Asher, and P. M. Champion. 1994. Determination of CO orientation in myoglobin by single crystal infrared linear dichroism. *J. Am. Chem. Soc.* 116: 4139–4140

Jentzen, W. 1994. Strukturelle Heterogenität von Nickel-Octaethylporphyrin in nichtkoordinativen Lösungsmitteln. Doktorarbeit, Universität Bremen.

Kitagawa, T. 1988. Heme protein structure and the iron histidine stretching mode. *In* Biological Application on Raman Spectroscopy. T. G. Spiro, editor. John Wiley & Sons, New York. 97–132.

Knapp, E. W., S. F. Fischer, and F. Parak. 1983. The influence of protein dynamics on Mössbauer spectra. *J. Chem. Phys.* 78:4701–4711.

Leone, M., A. Cupane, V. Militello, and L. Cordone. 1994. Thermal broadening of the soret band in heme complexes and in heme proteins: role of the iron dynamics. *Eur. Biophys. J.* 23:349–352.

Loncharich, R. J., and B. R. Brooks. 1990. Temperature dependence of dynamics of hydrated myoglobin. Comparison of force field calculations with neutron scattering data. *J. Mol. Biol.* 215:439–455.

Makinen, M. W., R. A. Houtchens, and W. S. Caughey. 1979. Structure of carbonmonoxymyoglobin in crystals and in solution. *Proc. Natl. Acad. Sci. USA.* 76:6042–6046.

Miyazaki, Y., T. Matsuo, and H. Suga. 1993. Glass transition of myoglobin crystal. *Chem. Phys. Lett.* 213:303–308.

Morikis, D., P. M. Champion, B. A. Springer, and S. G. Sligar. 1989. Resonance raman investigations of site directed mutants of myoglobin: effects of distal histidine replacement. *Biochemistry.* 28:4791–4800.

Mourant, J. R., D. P. Braunstein, K. Chu, H. Frauenfelder, G. U. Nienhaus, P. Ormo, and R. D. Young. 1993. Ligand binding to heme proteins. II. Transitions in the heme pocket of myoglobin. *Biophys. J.* 65: 1496–1507.

Mrevlishvili, G. M. 1979. Low-temperature calorimetry of biological macromolecules. *Sov. Phys. Usp.* 22:433–455.

Nienhaus, G. U., J. R. Mourant, and H. Frauenfelder. 1992. Spectroscopic evidence for conformational relaxation in myoglobin. *Proc. Natl. Acad. Sci. USA.* 89:2902–2906.

Nienhaus, G. U., J. R. Mourant, K. Chu, and H. Frauenfelder. 1994. Ligand binding to heme proteins. V. The effect of light on ligand binding in myoglobin. *Biochemistry.* 33:13413–13430.

Ormos, P., D. Braunstein, H. Frauenfelder, M. K. Hong, A.-L. Lin, T. B. Sauke, and R. D. Young. 1988. Orientation of carbon monoxide and structure-function relationship in carbonmonoxymyoglobin. *Proc. Natl. Acad. Sci. USA.* 85:8492–8496.

Parak, F. 1986. Correlation of protein dynamics with water mobility: Mössbauer spectroscopy and microwave absorption. *Methods Enzymol.* 127:196–206.

Parak, F., E. W. Knapp, and D. Kucheida. 1982. Protein dynamics. Mössbauer spectroscopy on deoxymyoglobin crystals. *J. Mol. Biol.* 161: 177–194.

Perrson, B. N. J., and R. Ryberg. 1989. Vibrational line shapes of low-frequency adsorbate modes. *Phys. Rev. B.* 40:10273–10281.

Phillips, S. E. V. 1981. The x-ray structure of deoxyMb (pH = 8.5) at 1.4 Å resolution. Brookhaven Protein Data Bank., Brookhaven (USA).

Post, F., W. Doster, G. Karvounis, and M. Settles. 1993. Structural relaxation and nonexponential kinetics of CO-binding to horse myoglobin: multiple flash photolysis experiments. *Biophys. J.* 64:1833–1842.

Powers, L., B. Chance, M. Chance, B. F. Campbell, J. M. Friedman, S. Khalid, C. Kumar, A. Naqui, K. S. Reddy, and Y. Zhou. 1987. Kinetic, structural and spectroscopic identification of geminate states of myoglobin: a ligand site on the reaction path. *Biochemistry.* 26: 4785–4796.

Rosenfeld, Y. B, and S. S. Stavrov. 1994. Anharmonic coupling of soft modes and its influence on the shape of the iron-histidine resonance Raman band of heme proteins. *Chem. Phys. Lett.* 229:457–464.

Rousseau, D. L., and J. M. Friedman. 1988. Transient and cryogenic studies of photodissociated hemoglobin and myoglobin. *In* Biological Application on Raman Spectroscopy. T. G. Spiro, editor. John Wiley & Sons, New York. 133–216.

Sage, J. T., K. T. Schomaker, and P. M. Champion. 1995. Solvent-dependent structure and dynamics in myoglobin. *J. Phys. Chem.* 99: 3394–3405.

Sassaroli, M., S. S. Dasgupta, and D. L. Rousseau. 1986. Cryogenic stabilization of myoglobin photoproducts. *J. Biol. Chem.* 261: 13704–13713.

Schweitzer-Stenner, R. 1989. Allosteric linkage-induced distortions of the prosthetic group in haem proteins as derived by the theoretical interpretation of the depolarization ratio in resonance Raman scattering. *Q. Rev. Biophys.* 22:381–479.

Schweitzer-Stenner, R., and W. Dreybrodt. 1992. Investigation of haem-protein coupling and structural heterogenity in myoglobin and haemoglobin by resonance Raman spectroscopy. *J. Raman Spectrosc.* 23: 539–550.

Schweitzer-Stenner, R., W. Jentzen, and W. Dreybrodt. 1993a. Anharmonic coupling in nickel(II) octaethylporphyrin investigated by resonance Raman spectroscopy. *In* Fifth International Conference on the Spectroscopy of Biological Molecules. T. Theophanides, J. Anastassopoulou, and N. Fotopoulos, editors. Kluwer Academic Publishers, Drodrecht. 31–32.

Schweitzer-Stenner, R., M. Bosenbeck, and W. Dreybrodt. 1993b. Raman dispersion spectroscopy probes heme distortions in deoxyHb-trout IV involved in its T-state Bohr effect. *Biophys. J.* 64:1194–1209.

Singh, G. P., F. Parak, S. Hunklinger, and K. Dransfeld. 1981. Role of adsorbed water in the dynamics of proteins. *Phys. Rev. Lett.* 47: 685–688.

Šrajer, V., and P. M. Champion. 1991. Investigations of optical line shapes and kinetic hole burning in myoglobin. *Biochemistry.* 30:7390–7402.

Šrajer, V., L. Reinish, and P. M. Champion. 1988. Proteins fluctuation, distributed coupling and the binding of ligands to heme proteins. *J. Am. Chem. Soc.* 110:6656–6666.

Šrajer, V., L. Reinish, and P. M. Champion. 1991. Investigation of laser induced long-lived states of photolyzed MbCO. *Biochemistry.* 30: 4886–4895.

Šrajer, V., K. T. Schomaker, and P. M. Champion. 1986. Spectral broadening in biomolecules. *Phys. Rev. Lett* 57:1267–1270.

Stein, D. L. 1985. A model of protein conformational substates. *Proc. Natl. Acad. Sci. USA.* 82:3670–3672.

Stavrov, S. S. 1993. The effect of iron displacement out of the porphyrin plane on the resonance Raman spectra of heme proteins and iron porphyrins. *Biophys. J.* 65:1942–1950.

Stavrov, S. S., and B. Kushkuley. 1993. Dependence of the iron-histidine frequency of deoxy heme proteins on the structure of its active center: a quantum chemical study. *In* Proceedings of the Fifth European Conference on the Spectroscopy of Biological Molecules. T. Theophanides, editor. Kluwer, Amsterdam. 305–306.

Steinbach, P. J., and B. F. Brooks. 1993. Protein hydration elucidated by molecular dynamics simulation. *Proc. Natl. Acad. Sci. USA.* 90: 9135–9139.

Steinbach, P. J., A. Ansari, J. Berendzen, D. Braunstein, K. Chu, B. R. Cowen, D. Ehrenstein, H. Frauenfelder, J. B. Johnson, D. C. Lamb, S. Luck, J. R. Mourant, G. U. Nienhaus, P. Ormos, R. Phillip, A. Xie, and R. D. Young. 1991. Ligand binding to heme proteins: connection between dynamics and function. *Biochemistry.* 30:3988–4001.

Steinhoff, H.-J., B. Kramm, G. Hess, C. Owerdiek, and A. Redhardt. 1993. Rotational and translational water diffusion in the hemoglobin hydration shell: dielectric and proton nuclear relaxation measurements. *Biophys. J.* 65:1486–1495.

Stryer, L. 1988. Biochemistry, 3rd ed. W. H. Freeman, San Francisco.

Tian, W. D., J. T. Sage, and P. M. Champion. 1992. Relaxation dynamics of myoglobin in solution. *Phys. Rev. Lett.* 68:408–411.

Zerner, M., M. Gouterman, and H. Kobayashi. 1966. Porphyrins. VII. Extended Hückel calculation on iron complex. *Theor. Chim. Acta.* 6:363–400.